



## Characterization of drug–protein binding process by employing equilibrium sampling through hollow-fiber supported liquid membrane and Bjerrum and Scatchard plots

Thaer Barri<sup>a,\*</sup>, Tatjana Trtić-Petrović<sup>b</sup>, Michael Karlsson<sup>a</sup>, Jan Åke Jönsson<sup>a</sup>

<sup>a</sup> Department of Analytical Chemistry, University of Lund, P.O. Box 124, SE-22100 Lund, Sweden

<sup>b</sup> Vinča Institute of Nuclear Sciences, Laboratory of Physics, P.O. Box 522, 11001 Belgrade, Serbia

### ARTICLE INFO

#### Article history:

Received 12 February 2008  
Received in revised form 25 April 2008  
Accepted 28 April 2008  
Available online 8 May 2008

#### Keywords:

Drug–protein binding  
Free concentration  
Equilibrium sampling through membrane  
Binding parameters  
Bjerrum and Scatchard plots

### ABSTRACT

The technique equilibrium sampling through membrane (ESTM) was extended to measuring the free drug concentration in solutions of drug and protein. Bjerrum and Scatchard plots were employed for characterizing individual drug binding to pure human blood proteins. Four drugs were investigated as a model system: fluvoxamine and ropivacaine which dominantly bind to  $\alpha$ -acid glycoprotein (AGP), and *R,S*-ibuprofen and *S*-ketoprofen which highly bind to human serum albumin (HSA). The level of drug binding to AGP and HSA relied on drug and protein concentrations. Bjerrum and Scatchard plots revealed high affinity constants ( $K_a$ ) at low protein concentration. Both Bjerrum and Scatchard plots of fluvoxamine and ropivacaine binding to AGP showed one specific binding site ( $n_1 = 1$ ) with ropivacaine  $K_a$  value close to 5 times higher than the  $K_a$  of fluvoxamine at 22.9  $\mu\text{M}$  AGP concentration. Bjerrum plots of ketoprofen and ibuprofen gave total number of binding sites or bound molecules of 6–7, which did not depend on the drug or protein concentration. Scatchard plots of ketoprofen and ibuprofen exhibited two binding sites ( $n_1$  and  $n_2$ ) at 0.15  $\mu\text{M}$  and 0.75  $\mu\text{M}$  HSA concentrations. On one hand, at 0.15  $\mu\text{M}$  HSA, ketoprofen and ibuprofen were bound to site I at  $n_1 = 1.2$  and  $n_1 = 1.0$ , respectively. However, at 0.75  $\mu\text{M}$  HSA, ketoprofen and ibuprofen were bound to site I at  $n_1 = 1.2$  and  $n_1 = 1.9$ , respectively. On the other hand, site II, at 0.15  $\mu\text{M}$  HSA, interacted with ketoprofen and ibuprofen at  $n_2 = 5.6$  and 6.7, respectively. However, at 0.75  $\mu\text{M}$  HSA, site II interacted with ketoprofen at  $n_2 = 7.4$  and ibuprofen at  $n_2 = 6.2$ . It would be concluded that, upon mixing ketoprofen and ibuprofen in a HSA solution, a ketoprofen–ibuprofen interaction would most likely occur at site II in HSA.

© 2008 Elsevier B.V. All rights reserved.

### 1. Introduction

Noncovalent biomolecular interactions widely exist in nature and their binding parameters are fundamentally important in all binding studies of ligand–receptor nature. Characterization of the binding process by estimating the binding parameters, such as binding/association constant and number of binding sites and bound ligand molecules, is essential for understanding interactions (ligand–receptor, antigen–antibody and drug–protein) in the biological system. The measurement of the binding parameters of a drug bound to blood proteins is of utmost importance for drug discovery and preclinical studies of drug candidates in pharmaceutical research [1].

Most drugs extensively bind to two major blood proteins, human serum albumin (HSA) and  $\alpha_1$ -acid glycoprotein (AGP). HSA binds

mostly acidic and neutral drugs, while AGP binds basic and neutral drugs and many other molecules like steroid hormones [2]. The extent to which binding occurs varies and depends on the affinity between the drug and the protein, the drug and protein concentration, the medium pH, number and nature of the binding sites, the relative abundance of protein variants, and the presence of other substances, which either compete with the drug for the binding sites or displace it through allosteric effects.

HSA is the most abundant protein in mammals, which constitutes up to 60% with a plasma concentration range in human adult from 30 to 50  $\text{mg mL}^{-1}$  [3]. It has several different binding sites (I–VI) [4]. Each binding site has several binding regions, where interactions with drugs can occur and, therefore, one binding site can fit several drug molecules. Two of these binding sites, “site I” =  $n_1$  (warfarin site) and “site II” =  $n_2$  (benzodiazepine site), do have high drug binding affinities [5–7]. Known drugs to interact with “site I” are warfarin, azapropazone, phenylbutazone, indomethacin, iodipamide [5,8]. Binding “site II” has a high

\* Corresponding author. Tel.: +46 46 2220369; fax: +46 46 2224445.  
E-mail address: [thaer.barri@analykem.lu.se](mailto:thaer.barri@analykem.lu.se) (T. Barri).

affinity to aromatic carboxylic acids, for example, non-steroidal anti-inflammatory drugs [5,9].

AGP does have a low *pI* value (2.3–3.8), a high carbohydrate content ( $\approx 45\%$ ), and its adult human serum concentration is  $0.5\text{--}1\text{ mg mL}^{-1}$ . Recent investigations have indicated the presence of two separate drug-binding sites on AGP, one with high and the other with low affinity for binding drugs and steroids with different specificity and localization. In addition, five other binding sites, mostly with weak affinity, have been identified for binding of endogenous substances and drugs [2].

In addition to equilibrium dialysis and ultrafiltration, several modern analytical techniques, such as affinity capillary electrophoresis [10], high-performance affinity chromatography [11], fluorescence spectroscopy [12], surface plasmon resonance-based biosensor technology [13], and solid phase microextraction [14], have been widely applied for investigation of drug–protein binding (DPB) process. Membrane extraction techniques have been used for quantifying total drug extraction from plasma [15] and for evaluating the extent of DPB in plasma samples [16,17] by using the equilibrium sampling through membrane (ESTM) technique [18]. Some of the demerits of the aforementioned non-membrane-based techniques can be seen as that, firstly, the universality of fluorescence spectroscopy is questionable because tryptophan residues reflect only a portion of the potential binding sites to both AGP and HSA. Secondly, surface plasmon resonance technology [13], such as a Biacore™, based on HSA and AGP biosensor chips can be applied for determination of binding constants, but the need to purchase Biacore™ instrumentation as well as instrument and chip synthesis proficiency can be potential limitations [19]. Experimental artifacts associated with some of these techniques, in addition to the non-physiological conditions, affect drug and drug–protein equilibria and, thus, lead to erroneous results in DPB studies.

The aim of the present study was to investigate the binding parameters of drugs to plasma proteins by employing Bjerrum and Scatchard plots after measuring the free drug concentrations by applying the ESTM technique in a single hollow fibre under nondisturbed equilibrium and physiological conditions. Two major extensively binding biomacromolecules, HSA and AGP, were investigated as binding proteins. Four human drugs were used as model compounds, two of which were basic (fluvoxamine and ropivacaine) that mainly bind to AGP and the other two were acidic (*S*-ketoprofen and *R,S*-ibuprofen) that highly bind to HSA.

## 2. Theoretical background

### 2.1. Estimation of drug–protein binding parameters

Binding of a drug to a protein involves multiple binding equilibria that are complex in nature. Thus, these equilibria can be described by different equilibrium constants. From a macroscopic view, the equilibrium constants can be interpreted as stoichiometric equilibrium binding constants. However, the microscopic point of view of DPB can be more centered on the binding constants that are site-oriented, where each site has a site equilibrium constant [20].

By implementing the simple macroscopic view, a protein can have several independent specific binding sites, which exhibit the same or different affinity for a drug molecule. Also, there is another class of binding sites that do not specifically interact with the drug. The specific reversible binding interaction between a drug (*D*) and a protein (*P*) can be described generally by Eq. (1).



where subscript ‘f’ denotes a free (unbound) concentration. The thermodynamic binding/association ( $K_a$ ) constant is given by Eq. (2).

$$K_a = \frac{[D_nP]}{[D_f]^n [P_f]} \quad (2)$$

The total number of drug molecules bound to one molecule of protein, *r*, can be expressed as in Eq. (3).

$$r = \frac{[D_nP]}{[P_{\text{tot}}]} = \frac{[D_{\text{tot}} - D_f]}{[P_{\text{tot}}]} = \frac{[n_{\text{tot}}^D - n_f^D]}{[n_{\text{tot}}^P]} \quad (3)$$

Where  $D_{\text{tot}}$  is the total drug concentration and  $n_{\text{tot}}^D$ ,  $n_{\text{tot}}^P$  and  $n_f^D$  are the total number of moles of drug and protein and the number of moles of free drug, respectively.

By applying the ESTM technique, the concentration of free and bound drug can be easily determined under equilibrium conditions and without causing any shift in the thermodynamic equilibrium between the drug and the protein. However, the concentration of an unbound protein in equilibrium with bound protein is not possible to determine experimentally. Therefore, Eq. (2) can be modified by including the total concentration of protein;  $P_{\text{tot}}$ , as given in Eq. (4).

$$[P_{\text{tot}}] = [P_f] + [D_nP] \quad (4)$$

Then, Eqs. (2) and (4) can be re-arranged as shown in Eq. (5), which facilitates determination of  $K_a$  and *r* values:

$$\frac{[D_nP]}{[P_{\text{tot}}]} \equiv r = \sum_{i=1}^m \frac{n_i K_i [D_f]}{1 + K_i [D_f]} \quad (5)$$

Where *m*,  $n_i$  and  $K_i$  represent the number of classes of independent and non-interacting binding sites, the number of specific saturable binding sites and the binding constant, respectively.

Eq. (5) can be graphically presented in a form of Bjerrum plot in which the function of *r* versus  $\log D_f$  is obtained. This plot is characterized by a symmetrical S-shape with clearly recognizable inflection point. The value of *r* at the inflection point represents one half of the total number of bound molecules that are also equal to the specific saturable binding sites if the number of bound molecules and binding sites are equal. At this point,  $K_a$  is indicated by the reciprocal value of  $\log D_f$  on the abscissa. Additionally, Eq. (5) can be transformed to a form of Scatchard equation ( $r/[D_f] = nK_a - rK_a$ ), where  $r/[D_f]$  is plotted as a function of *r*. From this linearized function, the number of bound molecules per site, which should be equal to number of binding sites in the protein considering only one drug molecule binds to each site, is the *x*-intercept ( $n=r$ ) and the slope is equal to  $-K_a$ . This method of analyzing data has a disadvantage of introducing nonlinear errors by coordinate transformation, but it is still widely used in describing the DPB process. In case of one binding site or several binding sites with same affinity for the drug, Scatchard equation generates one straight line. Thus, in case of there are two binding sites with different affinity, these sites are represented by two lines each equivalent to a binding site [21]. The pitfalls of data evaluation from Bjerrum and Scatchard plots have been the concern of many research articles, for instance, the articles published by Brodersen et al. [22] and Šoltés et al. [23].

### 2.2. ESTM determination of free drug concentration

The theory of determining free drug concentration and level of DPB by applying ESTM was presented earlier [16,17], and below is only given a description of the theory.

In supported liquid membrane extraction, a three-phase system, analyte extraction and re-extraction processes occur simultaneously. The maximum concentration enrichment factor ( $E_{e(\text{max})}$ ) is

reached at equilibrium and can be expressed by Eq. (6).

$$E_{e(\max)} = \frac{C_A}{C_S} = \frac{\alpha_S K_S}{\alpha_A K_A} \quad (6)$$

where  $C_A$  and  $C_S$  are the final and initial concentrations of the acceptor and the sample solutions, respectively.  $K_A$  and  $K_S$  are the partition coefficients between the organic phase and the acceptor phase and the organic phase and sample phase, respectively.  $\alpha_A$  and  $\alpha_S$  are the fractions of the drug in uncharged form in the acceptor and sample phases, respectively. If the ionic strength and buffer composition of the sample and acceptor phases are similar, as the case in this work, then  $E_{e(\max)}$  will be equal to  $\alpha_S/\alpha_A$  as  $K_A$  and  $K_S$  will then be equal. Therefore, by carefully tuning the composition of the sample and acceptor phases, the  $E_e$  value and the system equilibrium can be manipulated.

When a protein solution contains a drug, two equilibria are established; the equilibrium between the drug–protein complex and free drug, and the equilibrium between charged (unextractable) and uncharged (extractable) drug molecules. If the extraction is performed at equilibrium conditions and the total concentration of the drug in the sample that is in equilibrium with the organic and the acceptor phase does not change significantly during the extraction, i.e. negligible depletion (not more than 5–10%) [24], then none of the equilibria will be influenced during the extraction. All of these equilibria are pH-dependent in the sample and acceptor phases. Considering an equilibrium between all phases in a drug/protein sample, the fraction of analyte in the extractable form in the sample,  $\alpha_S$ , has to be modified in order to include the effect of protein binding as it is stated in Eq. (7).

$$\alpha_S = \alpha_P \alpha_{Sd} \quad (7)$$

Where  $\alpha_P$  is the fraction of free extractable drug in a protein solution, and  $\alpha_{Sd}$  is the uncharged fraction of the non-bound (free) drug due to the dissociation equilibrium. Then, Eq. (7) for equilibrium-based extraction of a drug from a drug–protein solution can be re-written as in Eq. (8).

$$E_{e(\max)}^P = \frac{C_A^P}{C_S^P} = \frac{\alpha_P \alpha_{Sd} K_S^P}{\alpha_A K_A} \quad (8)$$

The superscript P denotes a protein solution. Dividing Eq. (8) by Eq. (6),  $\alpha_P$  can be quantitatively estimated as in Eq. (9).

$$\alpha_P = \frac{C_A^P \alpha_S K_S}{C_A \alpha_{Sd} K_S^P} \quad (9)$$

If the ionic strength and the buffer composition of the drug/buffer sample and drug/protein sample are similar, it can be assumed that  $\alpha_S = \alpha_{Sd}$  and  $K_S = K_S^P$ , and thus a simple equation for determination of the free fraction of a drug in a protein solution is obtained, that is  $\alpha_P = C_A^P/C_A$ . A very simple estimate of the percent of DPB can be obtained by measuring the analyte concentration in the acceptor solution after equilibrium extraction of the drug from both a protein solution ( $C_A^P$ ) and an aqueous buffer ( $C_A$ ) at the same total drug concentration. The experimentally obtained values of  $\alpha_P$  (free fraction) can be used for calculation of free drug concentration and level of DPB (%DPB =  $(1 - \alpha_P) \times 100$ ).

### 3. Experimental

#### 3.1. Chemicals and materials

Fluvoxamine maleate was obtained from Pharmacia & Upjohn S.p.A. (Milano, Italy). Ropivacaine hydrochloride was obtained from Astra Pain Pharmaceutical Production (Södertälje, Sweden). A 50/50 racemic mixture of ibuprofen, pure (S)-ketoprofen, human

AGP and fatty acid free HSA were purchased from Sigma–Aldrich (Steinheim, Germany). Dihexyl ether (DHE) and tri-octylphosphine oxide (TOPO) were purchased from Fluka (Steinheim, Germany). HPLC-grade methanol, triethylamine, phosphoric acid and analytical grade acetic acid (100% purity) were obtained from Merck (Darmstadt, Germany). All aqueous solutions were prepared in water purified by a Mili-Q/RO4 Millipore unit (Bedford, Massachusetts, USA). Buffer solutions of sodium phosphate were all of analysis grade and their salts were obtained from Merck. The polypropylene hollow-fibre membrane (ACCUREL PP50/280, Membrana GmbH, Wuppertal, Germany) had dimensions of “280  $\mu\text{m}$  I.D.  $\times$  50  $\mu\text{m}$  wall thickness  $\times$  0.1  $\mu\text{m}$  pore size”. The length was cut to 15 or 20 cm. The stock drug solutions (400  $\text{mg L}^{-1}$  fluvoxamine and ropivacaine and 500  $\text{mg L}^{-1}$  ibuprofen and ketoprofen) were prepared in phosphate buffer (pH 7.5; 67 mM) and were stable for at least 4 months when stored at 4 °C and protected from light. The aqueous working solutions were prepared daily from stock solutions.

#### 3.2. HPLC analysis

The HPLC system consisted of a pump (Varian 9012) and LC-detector (Spectroflow 755 ABI Analytical Kratos Division) operated at 210 nm for ropivacaine, 230 nm for fluvoxamine and 254 nm for ketoprofen. The column Ace 3 C<sub>18</sub> (250 mm  $\times$  4.6 mm, 3  $\mu\text{m}$ , Advanced Chromatography Technologies, Scotland) was used for ropivacaine and fluvoxamine analyses. The column LiChroCart C<sub>18</sub> (250 mm  $\times$  4 mm  $\times$  5  $\mu\text{m}$ ) protected by a C<sub>18</sub> guard pre-column (Phenomenex, Torrance, CA, USA) was used for ketoprofen analyses. The mobile phase for ropivacaine and fluvoxamine analyses was acetonitrile–triethylamine (10 mM aqueous solution) (33:67, v/v) (pH 2.90 adjusted by phosphoric acid) and pumped at a flow rate of 1  $\text{mL min}^{-1}$ . The sample volume was 2 mL. The calibration curves were done in a concentration range from 0.05 to 20  $\text{mg L}^{-1}$  with correlation coefficient ( $R^2$ ) of 0.9995 and 0.9998, and instrumental detection limits of 0.02 and 0.05  $\text{mg L}^{-1}$  for ropivacaine and fluvoxamine, respectively. The mobile phase used for ketoprofen analyses was methanol–water–acetic acid (75:25:1, v/v/v) and pumped at a flow rate of 0.8  $\text{mL min}^{-1}$ . Ketoprofen calibration curve was established in a concentration range of 0.05–5.0  $\text{mg L}^{-1}$  with  $R^2$  value of 0.9990. The HPLC data were evaluated by using Peak Simple software (SRI Instruments, Torrance, CA, USA). The HPLC system used for ibuprofen analyses consisted of a Hewlett Packard (HP) 1050 series pump and an LC detector (Agilent Technologies, CA, USA) used at 230 nm. The column was an Agilent zorbax C<sub>18</sub> (250 mm  $\times$  4.6 mm  $\times$  5  $\mu\text{m}$ ) protected by a Lichrosphere RP selectB (4 mm  $\times$  4 mm  $\times$  5  $\mu\text{m}$ ) guard column (Agilent Technologies). The mobile phase was methanol–water–acetic acid (85:15:1, v/v/v) and pumped at a flow rate of 1  $\text{mL min}^{-1}$ . Ibuprofen calibration curve was prepared by using eight different concentrations covering the range of 0.05–10  $\text{mg L}^{-1}$ . The correlation coefficient of the linear curve was 0.9970. Data analyses were performed by using an HP Chemstation A.04.02 software. All data were evaluated by using Microsoft Excel. Processed data were organized in figures using Microcal™ Origin™ 5.0 or 7.0 (Northampton, Massachusetts, USA). The injected sample volume was in the range of 5–20  $\mu\text{L}$ .

#### 3.3. Drug–protein solution preparation

The experiments of ketoprofen and ibuprofen binding to HSA were performed at two HSA concentrations; 1 and 5  $\text{mg mL}^{-1}$  (0.15 and 0.75  $\mu\text{M}$ ). At 0.15  $\mu\text{M}$  HSA, the concentration range for ketoprofen was from 3.93 to 396  $\mu\text{M}$  and for ibuprofen it was from 5.14 to 477  $\mu\text{M}$ . At a high protein concentration of 0.75  $\mu\text{M}$ , the ketopro-



fen concentration was in a range of 19.8–790  $\mu\text{M}$  and the ibuprofen concentration range was from 24.6 to 1030  $\mu\text{M}$ .

Binding of fluvoxamine and ropivacaine to AGP was studied at 1 mg mL<sup>-1</sup> (22.9  $\mu\text{M}$ ) AGP concentration. At this protein concentration, the fluvoxamine concentration range was studied from 0.6 to 540.9  $\mu\text{M}$  and the ropivacaine concentration from 2.4 to 325.3  $\mu\text{M}$ . AGP binding experiments at 0.5 mg mL<sup>-1</sup> (11.45  $\mu\text{M}$ ) were only carried out for ropivacaine at concentration range from 1.8 to 165.2  $\mu\text{M}$ .

The sample (protein or buffer solution that contains the individual drug) was prepared in phosphate buffer (pH 7.5; 67 mM). The sample was a 2-mL mixture of 1:1 protein and drug solutions. The acceptor solution was phosphate buffer (67 mM, pH 7.05–7.5 depending on the drug). The extraction equilibrium time was 60 min for ropivacaine and fluvoxamine [17] and 90 min for ibuprofen and ketoprofen (experimentally determined). The measurement was done in two parallel sets of samples of protein and buffer solutions, each containing the same total drug concentration (both in triplicate).

#### 3.4. ESTM extraction in a single hollow fiber

Fig. 1 depicts how a short piece of a hollow-fiber membrane was employed as an extraction device in ESTM. A 0.5-mL micro-fine syringe (a) attached to a needle of 0.30-mm outer diameter and 8-mm length (obtained from BD Consumer Healthcare, NJ, USA) was used to fill the acceptor solution into the lumen of a hollow-fiber membrane (b) for extraction and to flush out the acceptor

solution into a small glass vial after extraction (c). The membrane was then impregnated by soaking in the organic phase for 5–15 s, which was followed by washing the outer membrane surface in water. The organic solvent was DHE (for ibuprofen and ketoprofen experiments) or 5% (w/v) TOPO in DHE (for fluvoxamine and ropivacaine experiments). Then, the lumen of the hollow fiber was washed with acceptor buffer. Both ends of the hollow fibre were put together to form a loop, sealed by bending the two ends over and fixing with aluminium foil and finally attached to a 50- $\mu\text{L}$  vial glass insert (Alltech Associates, Inc., IL, USA).

The fibre loop (d) was put into a 4-mL sample vial filled with 2 mL of sample as can be seen in (e) with enlarged view of it in (f). During the extraction, the sample vial was shaken at 100 or 130 rpm by using a shaker (INFORS AG, Bottmingen, Switzerland). After a pre-determined equilibrium time of extraction, the acceptor phase containing the free drug was collected by pressing the content of the lumen into a glass vial insert with help of the microsyringe, followed by extract injection (5 or 10  $\mu\text{L}$ ) into the HPLC after a proper dilution if needed.

## 4. Results and discussion

### 4.1. Drug–protein binding determination

The method used for determination of DPB parameters in this study was based on the ESTM technique in a single hollow fibre. The experimental conditions were tuned so as to achieve incomplete trapping in the acceptor buffer phase. Incomplete trapping can be reached by either adjusting the sample or acceptor pH values. In this work, the sample pH was buffered and maintained at 7.5, mimicking the physiological plasma pH. Therefore, incomplete trapping was achieved by manipulating the acceptor pH values (pH 7.05 and 7.2 for fluvoxamine and ropivacaine, respectively) [17]. The ionic strength in the sample and acceptor solutions was equal to the physiological values. At wide drug concentration range, the impact of protein concentration on the binding parameters was evaluated. The influence of the total fluvoxamine and ropivacaine concentration on the percent of drug–AGP binding is illustrated in Fig. 2. The concentration of AGP was kept constant in these experiments and equal to the concentration in the human healthy blood plasma, 1 g dm<sup>-3</sup> (22.9  $\mu\text{mol dm}^{-3}$ —calculated on the basis of different molecular weight of AGP reported in literature [2]). It can be seen in Fig. 2(i) that the DPB of fluvoxamine was highly dependent on total drug concentration. When the total drug concentration was increased in the sample, the level of DPB decreased. This decrease was rapid at low drug concentration. For example, at fluvoxamine concentration range of 0.60–46  $\mu\text{M}$ , DPB declined from 70 to 18%. However, upon further increase in total drug concentration, DPB dropped very slowly (from 18 to 5% at drug concentration of 45–540.9  $\mu\text{M}$ ). Somewhat similar values of DPB of fluvoxamine to whole plasma sample were obtained, decreasing from 70 to 45% at concentration range from 0.57 to 5.3  $\mu\text{M}$  [17].

The dependence of DPB of ropivacaine on total drug concentration is given in Fig. 2(ii). Two concentrations of AGP (22.9 and 11.45  $\mu\text{M}$ ) were investigated for similar concentrations of ropivacaine. When ropivacaine concentration was gradually increased, the DPB markedly decreased. This dependence was similar to fluvoxamine behavior. For instance, at low drug concentration range of 2.4–40  $\mu\text{M}$ , the DPB rapidly declined from 76 to 25%. However, the DPB much slowly decreased (25–7%) at total drug concentration of 40–325  $\mu\text{M}$ .

Comparing the results of DPB at two AGP concentrations and the same total ropivacaine concentration, the DPB was higher at high AGP concentration. For example, at 45  $\mu\text{M}$  ropivacaine, the DPB was 20 and 31% at 11.45 and 22.9  $\mu\text{M}$  AGP concentrations, respectively.

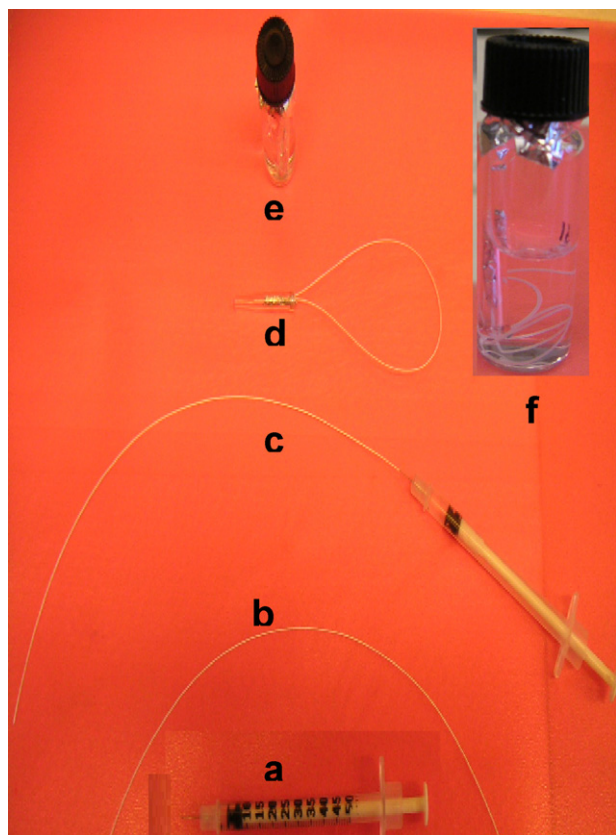
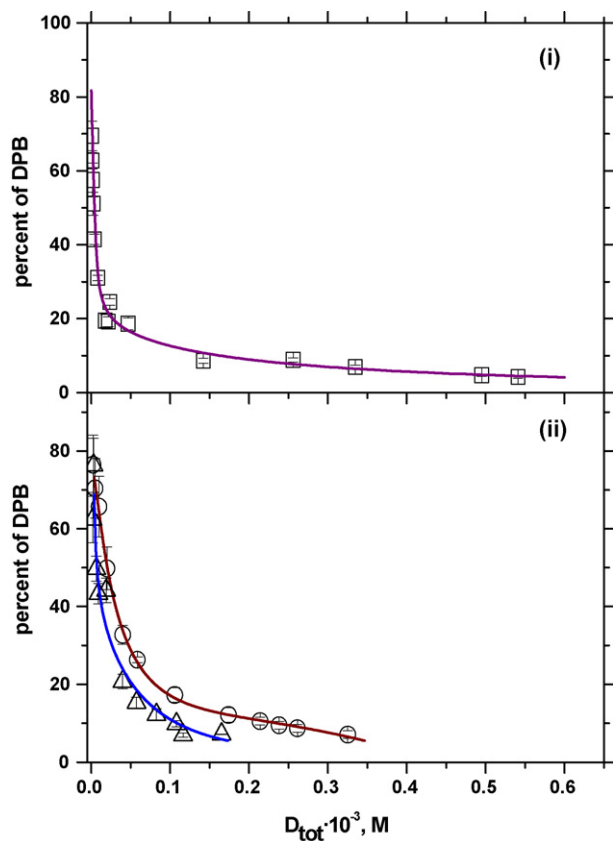


Fig. 1. Handling the hollow fiber and solutions in the ESTM technique. From the bottom: (a) a 0.5-mL microsyringe, (b) a short piece of a hollow fiber, (c) a hollow fiber attached to a 0.5-mL microsyringe, (d) a sealed fiber loop, (e) a 4-mL sample vial containing 2 mL of sample solution and a sealed hollow fiber and (f) an enlarged view of (e).



**Fig. 2.** The influence of total drug concentration of fluvoxamine and ropivacaine on AGP binding (%DPB). (i) Fluvoxamine at AGP concentration of (□) 22.9  $\mu\text{M}$  and (△) Ropivacaine at AGP concentration of (○) 22.9  $\mu\text{M}$  and (△) 11.45  $\mu\text{M}$ .

This difference in DPB was less significant at low total drug concentration. In addition, looking at the DPB values of ropivacaine obtained from plasma [17] and AGP samples, one can see that, at concentration range from 2.3 to 32.5  $\mu\text{M}$ , the DPB decreased slower (74–60%) in plasma than in pure protein solution (76–36%). However, the DPB at the lowest investigated ropivacaine concentration was almost the same in plasma and pure AGP solution, but differences were obtained at high concentration of ropivacaine. It could be probably derived from additional binding of ropivacaine to HSA [25]. These results showed that both drug and protein concentrations do have an impact on the DPB level. This can be important in case of a dose drug determination.

The impact of total drug concentration of ibuprofen and ketoprofen on the percent of drug bound to HSA is illustrated in Fig. 3. At 0.15  $\mu\text{M}$  HSA concentration and gradually increasing total drug concentration from 3.93 to 396  $\mu\text{M}$  for ketoprofen and from 5.14 to 477  $\mu\text{M}$  for ibuprofen, the DPB drastically reduced from 84 to 25% for ketoprofen (Fig. 3 open circles) and from 94 to 22% for ibuprofen (Fig. 3 open triangles).

However, DPB at high protein concentration (0.75  $\mu\text{M}$ ) much smoothly declined. At this HSA concentration, an increase in total ketoprofen concentration from 19.8 to 790  $\mu\text{M}$  only reduced the DPB from 92 to 56% (Fig. 3 black circles) and an increase in total ibuprofen concentration from 24.6 to 1030  $\mu\text{M}$  reduced DPB from 96 to 51% (Fig. 3 black triangles). This demonstrates that a five-time increase in protein concentration at 394  $\mu\text{M}$  ketoprofen and 477  $\mu\text{M}$  ibuprofen indicated a binding site saturation of 3 times for ketoprofen and 4 times for ibuprofen. This also suggests that the relationship between protein concentration and the level of DPB is not linear. It can be anticipated that, at very high HSA concen-

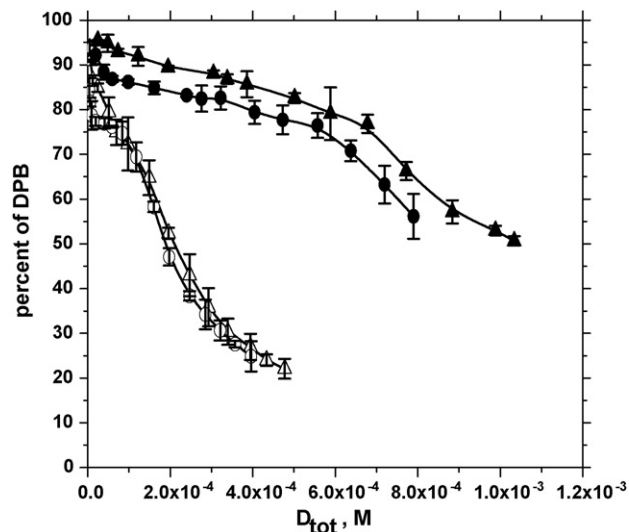


**Fig. 3.** The impact of total drug concentration of ibuprofen and ketoprofen on HSA binding (%DPB). Ketoprofen at HSA concentration of (●) 0.75  $\mu\text{M}$  and (○) 0.15  $\mu\text{M}$  and Ibuprofen at HSA concentration of (▲) 0.75  $\mu\text{M}$  and (△) 0.15  $\mu\text{M}$ .

tration (i.e. biological concentration (30–50  $\text{mg mL}^{-1}$ )), the drugs would be extensively bound to HSA at any drug concentration. It is also interesting to see that, at low HSA concentration, there was no significant difference in protein binding between *S*-ketoprofen and *S/R*-ibuprofen. On contrary, at high HSA concentration, this difference was markedly increased. Moreover, it can be seen from Fig. 3 that the initial decrease in DPB was followed by a plateau and then followed by another significant decrease, with exception of ibuprofen binding at 0.15  $\mu\text{M}$  HSA. This would suggest that HSA contains two binding sites (“site I” =  $n_1$  and “site II” =  $n_2$ ) with different affinity for the model compounds. This is a semi-qualitative evidence of presence of both sites that are available for drug binding. Also, it is evident from Fig. 2 (curve without any plateau) that only one binding site was present in AGP for binding fluvoxamine and ropivacaine.

## 4.2. Drug–protein binding parameters

### 4.2.1. Bjerrum plots

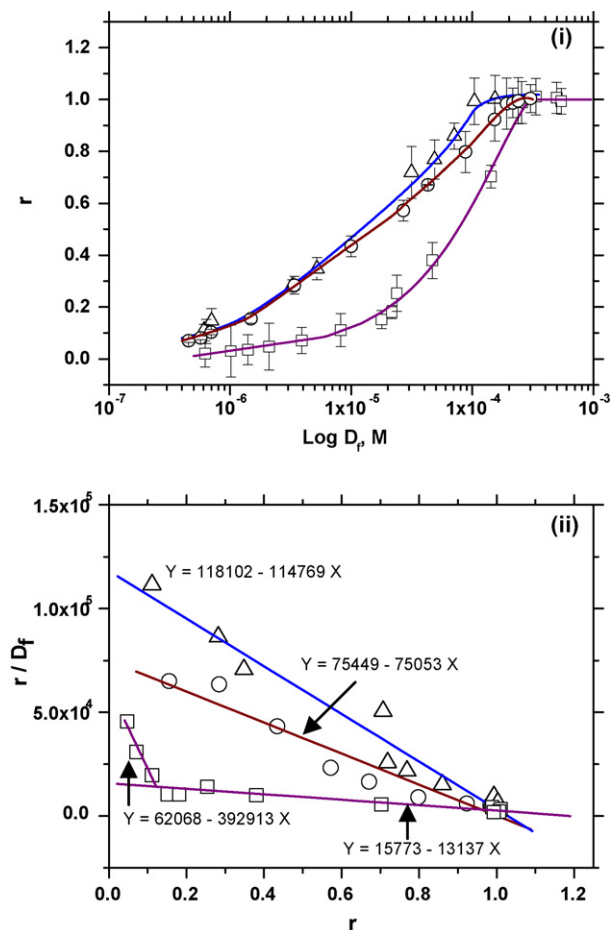
The determination of free and bound drug concentrations at undisturbed equilibrium conditions is the basis for estimating the DPB parameters. A Bjerrum plot for fluvoxamine binding to AGP is shown in Fig. 4(i). It is clear from this figure that one saturable binding site for one drug molecule was available in AGP for fluvoxamine binding. The obtained  $K_a$  value is shown in Table 1.

Fig. 4(i) also shows two Bjerrum plots for ropivacaine binding to two AGP concentrations. It can be seen from both plots that AGP had also one saturable binding site for ropivacaine and only one molecule of drug was bound to AGP. The  $K_a$  values at two AGP concentrations are shown in Table 1. The value of  $K_a$  was slightly higher at low (11.45  $\mu\text{M}$ ) than at high (22.9  $\mu\text{M}$ ) AGP concentration. The  $K_a$

**Table 1**

The drug–AGP binding parameters of fluvoxamine and ropivacaine obtained from Bjerrum and Scatchard plots in Fig. 4

Drug	[AGP] ( $\mu\text{M}$ )	Bjerrum plot		Scatchard plot	
		$K_a \times 10^4$ ( $\text{M}^{-1}$ )	$r_{\text{max}} = n_{\text{tot}}$	$K_a \times 10^4$ ( $\text{M}^{-1}$ )	$n$
Fluvoxamine	22.9	1.309	1	1.313	1
	11.45	6.531	1	7.545	1
Ropivacaine	22.9	8.066	1	11.477	1



**Fig. 4.** (i) Bjerrum plots of fluvoxamine and ropivacaine: Fluvoxamine at AGP concentration of (□) 22.9 μM and Ropivacaine at AGP concentration of (○) 22.9 μM and (△) 11.45 μM. (ii) Scatchard plots of fluvoxamine and ropivacaine: Fluvoxamine at AGP concentration of (□) 22.9 μM and Ropivacaine at AGP concentration of (○) 22.9 μM and (△) 11.45 μM.

value of ropivacaine was 5 times higher than that for fluvoxamine at 22.9 μM AGP concentration.

Bjerrum plots for ketoprofen and ibuprofen at two different HSA concentrations are depicted in Fig. 5. The binding parameters from Bjerrum plots are summarized in Table 2, where one can see that a 5-time increase in HSA concentration resulted in 3 and 2 times decrease in  $K_a$  for ketoprofen and ibuprofen, respectively. This proves that protein concentration influences  $K_a$  in an unpredictable manner. Thus, in protein binding experiments, the protein concentration should be fixed at an established known level and it would be highly important to define standardized experimental conditions as suggested by Deschamps-Labat et al. [26]. In addition, this indicates that the assumptions that both drugs interact with the same binding site; "site II", are correct. Also, the total number of bound molecules for ibuprofen ( $r_{ibu}$ ) agreed very well with the total

**Table 2**  
The drug–HSA binding parameters of ketoprofen and ibuprofen extracted from Bjerrum plots in Fig. 5

Drug	[HSA]		[HSA]	
	0.15 μM		0.75 μM	
	$r_{max} = n_{tot}$	$K_a \times 10^5 (M^{-1})$	$r_{max} = n_{tot}$	$K_a \times 10^5 (M^{-1})$
Ketoprofen	6.6	0.62701	6.5	0.18665
Ibuprofen	7.2	0.56405	7.2	0.24464

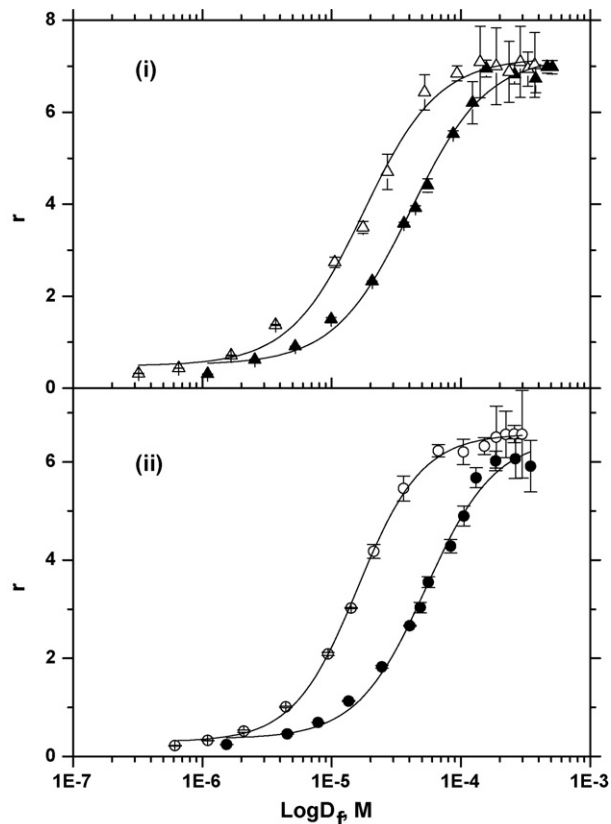


**Fig. 5.** Bjerrum plots of ibuprofen and ketoprofen: (i) Ibuprofen at HSA concentration of (▲) 0.75 μM and (△) 0.15 μM and (ii) Ketoprofen at HSA concentration of (●) 0.75 μM and (○) 0.15 μM.

number of bound molecules that are found in scientific literature ( $n_1 + n_2 = 5.3–7.1$ ) [5,26–28]. While for ketoprofen, the total number of bound molecules ( $r_{keto}$ ) was slightly lower than literature values ( $n_1 + n_2 = 8.5–9.4$ ) [26,29,30].

It can be noted that all of the fitted functions of Bjerrum plots in Fig. 4(i) and Fig. 5 were singly S-shaped, indicating that the individual drug interacts with only one binding site (Fig. 4(i)) or more binding sites with the same affinity (Fig. 5). Another observation from these figures was that, as AGP and HSA concentration was increased, the curves shifted to the right; i.e.  $K_a$  decreased. Bjerrum plots in Fig. 5 gave a total number of bound molecules of 6–7 for ketoprofen and 7 for ibuprofen. This suggests the presence of either one binding site or many binding sites that do have similar binding constant.

#### 4.2.2. Scatchard plots

Scatchard plots of fluvoxamine and ropivacaine binding to AGP are found in Fig. 4(ii). The  $K_a$  values and number of binding sites obtained from these plots are given in Table 1. Scatchard plots of fluvoxamine can be fitted with two lines, which would indicate presence of two binding sites, but  $r$  value of  $n_1 = 0.16$  would mean that the binding was non-specific. It can be seen from Table 1 that the  $K_a$  value ( $1.313 \times 10^4 M^{-1}$ ) agreed very well with the one obtained from Bjerrum plot. Unfortunately, there were no literature data available on the binding parameters of ropivacaine and fluvoxamine to AGP for comparing the results obtained.

It is clear in Fig. 4(ii) and Table 1 that only one molecule of ropivacaine was bound to one binding site of AGP molecule. The obtained values of  $K_a$  from Scatchard plots agreed well with those from Bjerrum plots. Although, the  $K_a$  value for ropivacaine was always higher



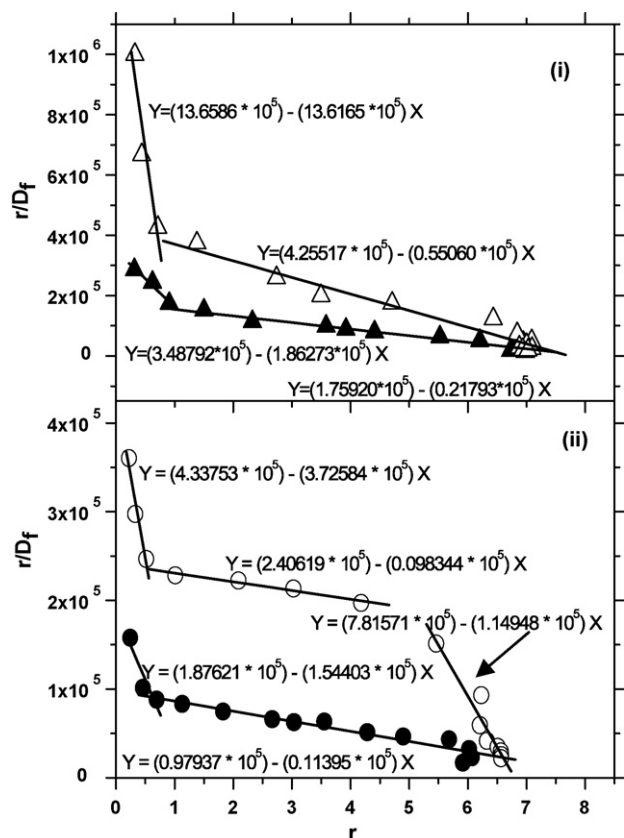


**Fig. 6.** Scatchard plots of ibuprofen and ketoprofen: (i) Ibuprofen at HSA concentration of ( $\Delta$ ) 0.15  $\mu\text{M}$  and ( $\blacktriangle$ ) 0.75  $\mu\text{M}$  and (ii) Ketoprofen at HSA concentration of ( $\circ$ ) 0.15  $\mu\text{M}$  and ( $\bullet$ ) 0.75  $\mu\text{M}$ .

at low than at high AGP concentration, the  $K_a$  difference at low and high AGP concentration was higher in Scatchard plots than those obtained from Bjerrum plot.

Scatchard plots found in Fig. 6 implied that both ketoprofen and ibuprofen had two binding sites ( $n_1$  and  $n_2$ ) on HSA with different  $K_a$  values. In this figure, each linear function represented drug interaction at one site in the protein. Therefore, at each protein concentration, two linear functions that cross  $x$ -axis (two sites) were found. Exceptionally, ketoprofen at 0.15  $\mu\text{M}$  HSA (Fig. 6(ii)) showed a third linear four-point semi-flat fit between the other two linear functions. This third middle function means that both free and bound concentrations had increased at total ketoprofen concentration range of 20  $\mu\text{M}$  to 84  $\mu\text{M}$ , but the ratio of  $r/D_f$  was more or less constant in that concentration range. This would mean that the third middle line could represent a “transition state” for ketoprofen molecules that are going to be bound to “site II”.

The  $K_a$  values and number of bound molecules per binding site are listed in Table 3. For ketoprofen bound to “site I”,  $n_1$  was 1.2 for both protein concentrations with different values of  $K_a$ . However, for ibuprofen bound to “site I”,  $n_1$  was 1.0 at low and 1.9 at high protein concentration with different values of  $K_a$ . On the other hand,

“site II” on HSA interacted with both model compounds binding 6 or 7 drug molecules. The number of bound molecules to both sites as well as the corresponding  $K_a$  values depended on HSA and drug concentration, with exception of ketoprofen molecules bound to “site I”.

These results explicitly showed that drug association to “site I” was always stronger (i.e. higher binding constant) than “site II” as well as it was stronger for both sites at low HSA concentration. For instance, ibuprofen binding to “site I” was 7 times stronger at 0.15  $\mu\text{M}$  than at 0.75  $\mu\text{M}$  HSA, while for ketoprofen it was 2 times higher. On contrary, ketoprofen association to “site II” was 10 times higher at 0.15  $\mu\text{M}$  than at 0.75  $\mu\text{M}$  HSA, while for ibuprofen it was 2 times higher. This reflects that ibuprofen interacts more favorably with “site I” than “site II”, and the opposite is true for ketoprofen. Furthermore, this would imply that “site I” (for ibuprofen) or “site II” (for ketoprofen) in HSA is more sensitive for a change in its microenvironment.

$K_{a1}$  of ibuprofen at 1 mg  $\text{mL}^{-1}$  (0.15  $\mu\text{M}$ ) HSA was in the range found in literature ( $4.35 \times 10^5 \text{ M}^{-1}$  to  $35.6 \times 10^5 \text{ M}^{-1}$ ) [5,26–28] and was three times higher than  $K_{a1}$  in Ref. [26] as well as one-half of the values reported in Refs. [27,28]. However,  $K_{a2}$  of ibuprofen at the same protein concentration was within the range of published data ( $0.0859 \times 10^5 \text{ M}^{-1}$  to  $1.5 \times 10^5 \text{ M}^{-1}$ ) [5,26–28] and was three times higher than the values found in Refs. [5,28]. It is also worth noting that the  $K_{a2}$  value of ibuprofen at 5 mg  $\text{mL}^{-1}$  (0.75  $\mu\text{M}$ ) HSA was very close to  $K_{a2}$  in Refs [5,28], being  $0.195 \times 10^5 \text{ M}^{-1}$  and  $0.178 \times 10^5 \text{ M}^{-1}$ , respectively. For ketoprofen, at 1 and 5 mg  $\text{mL}^{-1}$  HSA, the  $K_{a1}$  value was in the range of the published data ( $1.91 \times 10^5 \text{ M}^{-1}$  to  $4.92 \times 10^5 \text{ M}^{-1}$ ) [26,29,30] and was exactly equal to the value found in Ref. [29]. However, at 5 mg  $\text{mL}^{-1}$  HSA, the  $K_{a2}$  value of ketoprofen was not in the range found in literature ( $0.02 \times 10^5 \text{ M}^{-1}$  to  $0.05 \times 10^5 \text{ M}^{-1}$ ) [26,29,30].

From the binding behavior of ibuprofen and ketoprofen, it is very explicit that the number of ibuprofen molecules that preferably interacted with “site I” increased from 1.0 to 1.9 when HSA concentration was increased from 0.15 to 0.75  $\mu\text{M}$ . This could be explained by the observation that the number of ibuprofen molecules bound to site II (a relatively weak affinity site to ibuprofen compared to ketoprofen) decreased from 6.7 to 6.2 as HSA concentration was increased. One could predict that one molecule had moved to “site I” from “site II”. In the same manner, the number of ketoprofen molecules binding to “site II” increased from 5.6 to 7.4 when HSA concentration was increased from 0.15 to 0.75  $\mu\text{M}$ . As the number of ketoprofen molecules interacting with “site I” (a relatively weak affinity site to ketoprofen compared to ibuprofen) did not change, a more plausible explanation for this is that “site II” in HSA was able to cope with two more ketoprofen molecules at 0.75  $\mu\text{M}$  HSA. A reasonable explanation of this is that the allosteric effects might have happened, which could provide some conformational changes in the HSA structure, allowing a change in the number of drug molecules bound.

For ibuprofen, all literature values of number of bound ibuprofen molecules to HSA “site I” were equal or close to 1 [5,26–28], being very close to the value obtained in this work ( $n_1 = 1–2$ ). According to Scatchard plots in this work, the number of ibuprofen molecules bound to “site II” was 6.2 and 6.7 instead of 5–6 as it was stated in

**Table 3**

The drug–HSA binding parameters of ibuprofen and ketoprofen extracted from Scatchard plots in Fig. 6

Drug	[HSA]							
	0.15 $\mu\text{M}$				0.75 $\mu\text{M}$			
	$K_{a1} \times 10^5 \text{ (M}^{-1}\text{)}$	$n_1$	$K_{a2} \times 10^5 \text{ (M}^{-1}\text{)}$	$n_2$	$K_{a1} \times 10^5 \text{ (M}^{-1}\text{)}$	$n_1$	$K_{a2} \times 10^5 \text{ (M}^{-1}\text{)}$	$n_2$
Ketoprofen	3.72584	1.2	1.14948	5.6	1.54403	1.2	0.11395	7.4
Ibuprofen	13.6165	1.0	0.55060	6.7	1.86273	1.9	0.21793	6.2

the literature [5,26,28]. The number of ketoprofen molecules bound to “site I” was 1.2, which was very close to the literature values; being 1.4–2 [26,29,30]. The literature values of bound ketoprofen molecules to “site II” were between 7 and 8 [26,29,30], and were in the same magnitude as the results in Table 3.

It is important to keep in mind that the literature data were reported at different experimental conditions, such as HSA and drug concentrations, temperature and buffer solutions used, as well as the use of different analytical techniques applied. Therefore, this would be a reason for the minor differences in the results obtained in this work and literature data.

#### 4.2.3. Bjerrum versus Scatchard plots

The most important features of the results obtained from Bjerrum and Scatchard plots were that, firstly, Bjerrum plots only gave total number of molecules bound to the protein, suggesting either one binding site or many binding sites with similar affinity and one overall binding constant. In case of one binding site and one molecule binding to that site, representing the simplest system of drug–protein interaction (fluvoxamine and ropivacaine interaction with AGP), Bjerrum plot provided a very good approach of data analysis. However, Scatchard plots revealed more information about the number of molecules bound to each binding site and their respective binding constants. Secondly, ibuprofen and ketoprofen binding constants obtained from Bjerrum plots were equal to and 1.6 times higher than  $K_{a2}$  values from Scatchard plots, respectively, except that the  $K_{a2}$  of ketoprofen in Bjerrum plot at 0.15  $\mu\text{M}$  HSA was half of that in Scatchard plot. This would suggest that only binding at “site II” was visible in Fig. 5. Thirdly, the total number of ibuprofen molecules ( $r_{\text{ibu}}$ ) from Bjerrum plot was 7.2 at both HSA concentrations, and from Scatchard plot ( $n_1 + n_2$ ) was 7.7 and 8.1 at 0.15 and 0.75  $\mu\text{M}$  HSA concentration, respectively. This confirms our prediction of one more ibuprofen molecule was attached to “site I” when 0.75  $\mu\text{M}$  HSA was used. Similarly, the total number of ketoprofen molecules bound to HSA from Bjerrum plot ( $r_{\text{keto}}$ ) was 6.6 at both HSA concentrations. Whereas from Scatchard plot, ( $n_1 + n_2$ ) was 6.8 and 8.6 at 0.15 and 0.75  $\mu\text{M}$  HSA concentration, respectively.

## 5. Conclusion

Characterization of the drug–protein (AGP and HSA) binding process has been very successful by applying ESTM technique and employing Bjerrum and Scatchard plots. ESTM provided an easy-to-use tool for quantifying free drug concentration in a drug/protein mixture. The binding parameters were obtained by making use of the values of free drug concentration and Bjerrum and Scatchard plots. Fluvoxamine and ropivacaine binding to AGP represented a simple system for DPB studies. However, ketoprofen and ibuprofen exemplified a more complicated interaction with HSA. Shedding more light on this interaction, ketoprofen and ibuprofen binding to “site I” was always stronger than binding to “site II”. From Scatchard plots, the number of binding sites or bound molecules of ketoprofen and ibuprofen at  $n_1$  and  $n_2$  as well as the corresponding  $K_a$  values

relied on drug and HSA concentrations, with exception of ketoprofen at  $n_1$ . This implied that as drug and HSA concentrations were increased, the protein microenvironment was affected, and thus, site specific  $K_a$ ,  $n_1$  and  $n_2$  values were influenced. Therefore, from the binding behavior of ketoprofen and ibuprofen to HSA, it can be expected that, upon mixing simultaneously both drugs with HSA, a ketoprofen and ibuprofen competition for site II of HSA will most probably take place. In conclusion, the ESTM technique combined with Bjerrum and Scatchard plots can be used for characterizing any form of ligand–receptor interaction processes that are interesting for understanding biological systems.

## Acknowledgements

Tatjana Trtić-Petrović is indebted to Wenner-Gren Foundation, Sweden, for granting her a scholarship to carry out part of this work. This work was funded by the Swedish Science Research Council (VR). The authors also thank Ms. Nawroz Muhammed for helping in performing a few of the experiments.

## References

- [1] J. Oravcová, B. Böhs, W. Lindner, *J. Chromatogr. B* 677 (1996) 1–28.
- [2] Z.H. Israili, P.G. Dayton, *Drug. Metab. Rev.* 33 (2001) 161–235.
- [3] D.C. Carter, J.X. Ho, *Adv. Protein Chem.* 45 (1994) 153–203.
- [4] F. Hervé, S. Urien, E. Albengres, J.C. Duché, J.P. Tillement, *Clin. Pharmacokinet.* 26 (1994) 44–58.
- [5] T. Kosa, T. Maruyama, M. Otagiri, *Pharmaceut. Res.* 14 (1997) 1607–1612.
- [6] G. Sudlow, D.J. Birkett, D.N. Wade, *Mol. Pharmacol.* 12 (1976) 1052–1061.
- [7] G. Sudlow, D.G. Birkett, D.N. Wade, *Mol. Pharmacol.* 11 (1975) 824–832.
- [8] K.J. Fehske, U. Schläfer, U. Wollert, W.E. Müller, *Mol. Pharmacol.* 21 (1981) 387–393.
- [9] H. Wang, H. Zou, Y. Zhang, *Anal. Chem.* 70 (1998) 373–377.
- [10] M.H.A. Busch, L.B. Carels, H.F.M. Boelens, J.C. Kraak, H. Poppe, *J. Chromatogr. A* 777 (1997) 311–328.
- [11] D.S. Hage, *J. Chromatogr. B* 768 (2002) 3–30.
- [12] A. Sulkowska, *J. Mol. Struct.* 614 (2002) 227–232.
- [13] R.L. Riht, Y.S.N. Day, T.A. Morton, D.G. Myszyka, *Anal. Biochem.* 296 (2001) 197–207.
- [14] F.M. Musteata, J. Pawliszyn, *J. Proteome Res.* 4 (2005) 789–800.
- [15] T.S. Ho, S. Pedersen-Bjergaard, K.E. Rasmussen, *Analyst* 127 (2002) 608–613.
- [16] T. Trtić-Petrović, J.Å. Jönsson, *J. Chromatogr. B* 814 (2005) 375–384.
- [17] T. Trtić-Petrović, J.-F. Liu, J.Å. Jönsson, *J. Chromatogr. B* 826 (2005) 169–176.
- [18] J.-F. Liu, J.Å. Jönsson, P. Mayer, *Anal. Chem.* 77 (2005) 4800–4809.
- [19] L.H. Cohen, in: Z. Yan, G.W. Caldwell (Eds.), *Optimization in Drug Discovery: In Vitro Methods, Methods in Pharmacology and Toxicology*, Humana Press Inc., Totowa, NJ, 2004, pp. 111–122.
- [20] I.M. Klotz, D.L. Hunston, *J. Biol. Chem.* 250 (1975) 3001–3009.
- [21] S. Wei, L. Zhao, X. Cheng, J.-M. Lin, *Anal. Chim. Acta* 545 (2005) 65–73.
- [22] R. Brodersen, B. Honoré, A.O. Pedersen, I.M. Klotz, *Trends Pharmacol. Sci.* 9 (1998) 252–257.
- [23] L. Soltés, M. Mach, *J. Chromatogr. B* 768 (2002) 113–119.
- [24] M.B. Heringa, D. Pastor, J. Algra, W.H.J. Vaes, J.L.M. Hermens, *Anal. Chem.* 23 (2002) 5993–5997.
- [25] L. Simon, J.-X. Mazoit, *Baillieres Clin. Anaesthesiol.* 14 (2000) 641–658.
- [26] L. Deschamps-Labat, F. Péhourcq, M. Jagou, B. Bannwarth, *J. Pharm. Biomed. Anal.* 16 (1997) 223–229.
- [27] M.H. Rahman, T. Maruyama, T. Okada, T. Imai, M. Otagiri, *Biochem. Pharmacol.* 46 (1993) 1733–1740.
- [28] J.B. Whitlam, M.J. Crooks, K.F. Brown, P.V. Padersen, *Biochem. Pharmacol.* 28 (1978) 675–678.
- [29] D. Zhou, F. Li, *Se Pu.* 22 (2004) 601–604.
- [30] O. Borgå, B. Borgå, *J. Pharmacokinet. Biopharm.* 25 (1997) 63–76.